Internal boundary layers in the ocean circulation

Lecture 9 by Andrew Wells

We have so far considered boundary layers adjacent to physical boundaries. However, it is also possible to find boundary layers in the interior of the fluid domain. Two specific examples which we will discuss later are the oceanic thermocline and the equatorial undercurrent.

1 A simple example of an internal boundary layer: heat flow in a pipe

To demonstrate some of the characteristics of internal boundary layers we first consider a simple problem. Consider one-dimensional flow in a cylindrical pipe as shown in figure 1. The fluid is initially at a uniform temperature T_0 throughout the pipe, with flow at a constant velocity U along the length of the pipe. For time $t \geq 0$ the opening of the pipe is heated and maintained at a constant temperature T_1. The transfer of heat down the pipe can be described by the one dimensional advection-diffusion equation

$$\frac{\partial T}{\partial t} + U\frac{\partial T}{\partial x} = \kappa \frac{\partial^2 T}{\partial x^2}. \tag{1}$$

The thermal diffusivity κ is typically small, and so as a first approximation we might neglect the diffusion term on the right hand side of (1). This yields the solution

$$T = T_1 \qquad x - Ut \leq 0, \tag{2}$$
$$T = T_0 \qquad x - Ut > 0, \tag{3}$$

corresponding to a discontinuous jump in temperature propagating down the pipe at velocity U, as shown in figure 2(a). Clearly the discontinuity is unphysical, and we need an internal boundary layer

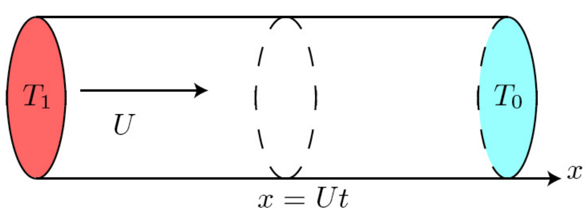

Figure 1: Fluid is pumped down a cylindrical pipe at a constant velocity U parallel to the pipe axis. The temperature is maintained at the constant value T_1 at the opening of the pipe at $x = 0$, with the remainder of the fluid initially at a temperature T_0.

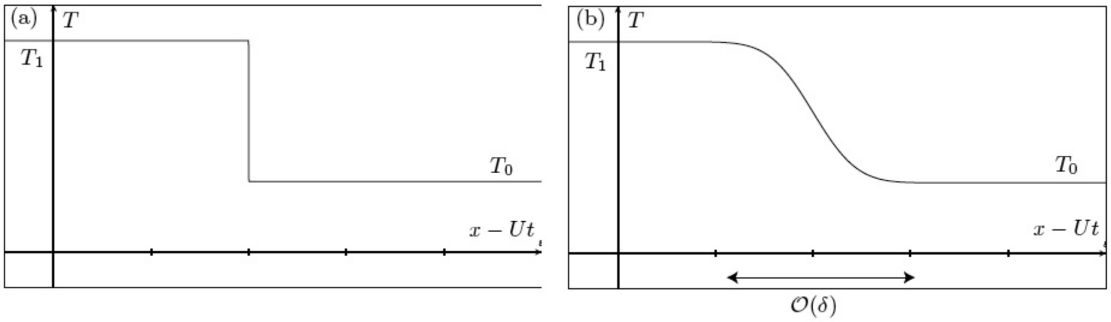

Figure 2: Snapshots of the temperature variation along the pipe, taken at a fixed value of t. (a) The solution in the absence of diffusion, showing a discontinuous jump in temperature. (b) The solution of the full advection diffusion equation. Diffusion acts to smooth the jump across an internal boundary layer of width $\delta = \mathcal{O}(\sqrt{\kappa t})$.

to smooth it out. The discontinuity arises due to the neglect of the diffusion term, mathematically giving a singular perturbation.

In this case we can obtain a solution of the full heat equation with the diffusion term included. We introduce a new system of co-ordinates moving with the shock, $\xi = x - Ut$ and $\tau = t$, so that (1) yields

$$\frac{\partial T}{\partial \tau} = \kappa \frac{\partial^2 T}{\partial \xi^2}. \tag{4}$$

In this reference frame, there are no imposed horizontal lengthscales and so we obtain the similarity solution

$$T = \frac{T_0 + T_1}{2} + \frac{T_0 - T_1}{2} \operatorname{erf}\left(\frac{\xi}{2\sqrt{\kappa\tau}}\right), \tag{5}$$

where the error function is defined as

$$\operatorname{erf}(x) = \int_0^x \exp\left(-u^2\right) \, du. \tag{6}$$

The full solution is plotted in figure 2(b), where we see that the jump in temperature has been smoothed out by diffusion over an internal boundary layer of width $\delta = \mathcal{O}(\sqrt{\kappa t})$. In the following discussion we will see that several structures of the ocean circulation are explained by the presence of internal boundary layers within the ocean.

2 The ventilated thermocline

The sub-tropical oceans have an interesting density profile, with a rapid variation in density over the upper kilometer of depth and a much weaker density gradient in the abyss at depths of 1 to 5.5 km. Typical density profiles in the Pacific Ocean are plotted in figure 3. The upper region of rapid variation, or *thermocline*, shows a distinct bowl-like shape in each hemisphere with the isopycnals sloping upward as we approach both poles and also as we approach the equator.

We outline a qualitative description of the dynamics here to motivate the detailed mathematical model presented in §2.1. The abyssal deep water beneath the thermocline is of polar origin and

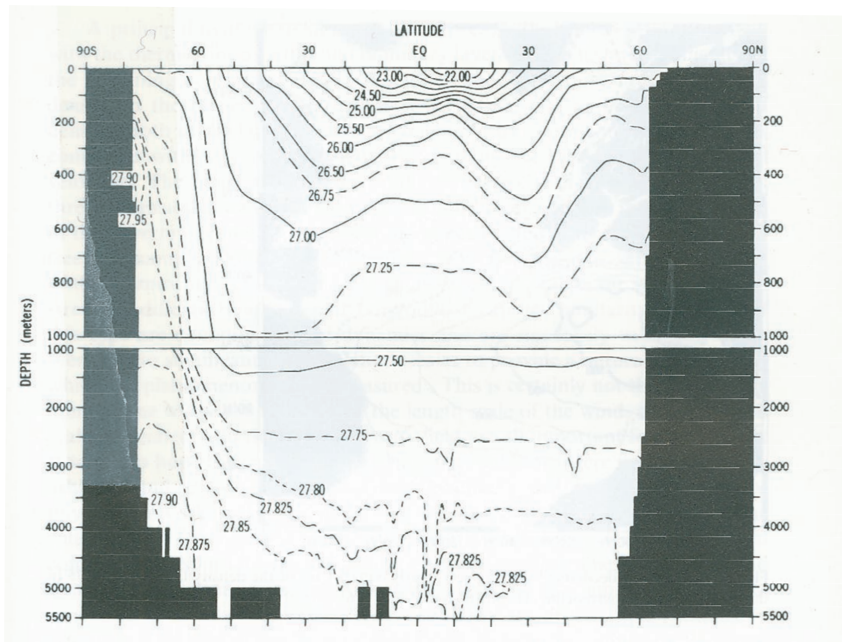

Figure 3: The zonally averaged potential density field for the Pacific Ocean. Note the change of vertical scale below 1000km reflecting the decrease in stratification below this depth. Image from Pedlosky (1998).

is thought to slowly upwell at mid-latitudes, establishing a temperature contrast with the warmer waters of the thermocline. The atmosphere imposes a temperature distribution on the surface of the ocean. This generates a decrease in surface density from the poles to the equator and hence the ispoycnals must intersect the surface. The surface wind stress in the sub-tropical gyres produces a downward Ekman pumping, carrying the surface density distribution downwards to generate a vertical density stratification. However, it is not immediately clear why we have an upwelling of the density distribution at low latitudes, creating a strongly stratified upper ocean close to the equator. By analogy with our pipe flow example, we might think of the downward pumping of the density distribution being interrupted in an internal boundary layer close to the equator, where a different dynamical balance takes over.

In the following section we develop a model of the ventilated thermocline, and use it to answer two principal questions:

1. Why does the isopycnal bowl become shallow at low latitudes?
2. Why does the surface forcing only penetrate to 1km?

2.1 The LPS model of the ventilated thermocline

Luyten et al. (1983) developed a model of the thermocline by considering the upper ocean as consisting of a series of layers of constant density. The entire wind driven circulation in the sub-tropical gyre is driven by a downward Ekman pumping of typical magnitude $w_e \approx 10^{-4}\mathrm{cm\,s^{-1}}$, generated by the wind shear stress exerted on the ocean surface. This is incorporated into the model by imposing an Ekman flux

$$w_e = \hat{\mathbf{k}} \cdot \nabla \times \frac{\tau}{\rho f}, \tag{7}$$

at the upper ocean surface as derived in a previous lecture (we do not resolve the upper mixed layer here.) We will consider a model with steady motion in two layers with thicknesses $h_1(x, y)$ and $h_2(x, y)$, lying above a deep abyss that is at rest. The structure and notation is illustrated schematically in figure 4. Note that the isopycnal at $z = -h_1$, marking the lower boundary of layer 1, outcrops at the latitude $y = y_2$ so that layer 2 is in contact with the surface forcing for $y > y_2$. This model is rather simplistic, but it describes the key characteristics of the circulation and it is possible to use it to construct a continuum model by resolving further layers.

2.1.1 Governing equations

We assume that the fluid flow is steady and effectively inviscid in the interior, with frictional effects confined to the surface Ekman layers and described by the imposed Ekman flux w_e. We treat the flow in each layer using inviscid shallow water theory, so that there is negligible frictional stress between the layers and no normal flow across the density interfaces. Applying mass conservation to each layer we obtain

$$\begin{aligned} \frac{\partial}{\partial x}(u_2 h_2) + \frac{\partial}{\partial y}(v_2 h_2) &= -w_e \qquad y > y_2, \\ &= 0 \qquad y < y_2, \end{aligned} \tag{8}$$

$$\frac{\partial}{\partial x}(u_1 h_1) + \frac{\partial}{\partial y}(v_1 h_1) = -w_e \qquad y < y_2. \tag{9}$$

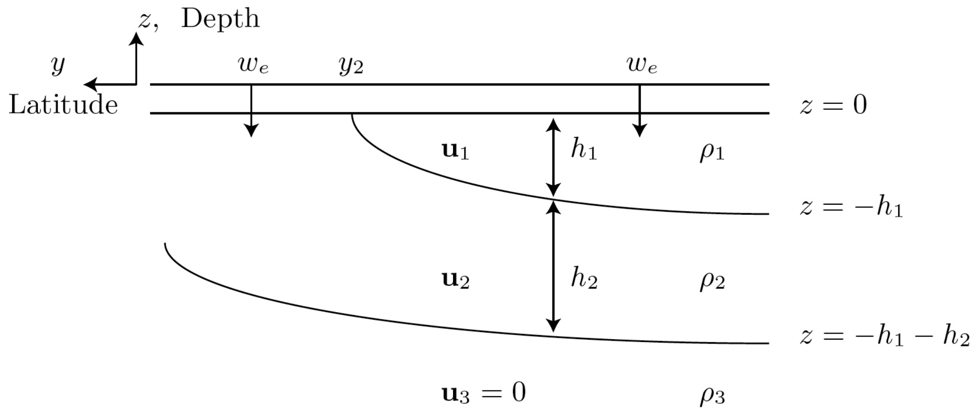

Figure 4: The two layer LPS model. The co-ordinates (x, y, z) vary with longitude, latitude and depth respectively. Fluid of density ρ_1 and pressure $p_1(x, y, z)$ flows with velocity $\mathbf{u}_1(x, y)$ in a layer $-h_1(x, y) < z < 0$. This overlies fluid of density ρ_2, pressure p_2 and velocity $\mathbf{u}_2$ in $-(h_1 + h_2) < z < -h_1$. The abyssal layer of density ρ_3 is at rest in $z < -(h_1 + h_2)$. The circulation is driven by an imposed Ekman downwelling velocity w_e.

In a steady state the horizontal mass flux in each layer changes only due to fluid input across the upper and lower interfaces. Hence each layer is fed by an Ekman pumping w_e while in contact with the free surface, and then after becoming submerged has no divergence of the horizontal mass flux because there is no normal flow across density interfaces.

In previous chapters we have seen that the dominant terms in the momentum balance will depend on the relevant scales for the problem. The Coriolis parameter is given by $f = 2\Omega \sin\theta$ where θ varies with latitude y. We let $\beta = \partial f/\partial y$ describe the variation of the Coriolis parameter with latitude. For a typical oceanic basin scale L and horizontal velocity U we have $U/\beta L^2 \ll 1$, so that the inertial scale is small relative to the basin scale. Alternatively we might think of this as implying that relative velocity gradients are small compared to planetary vorticity gradients. We can therefore neglect the non-linear advection terms, in addition to the viscous terms, so that the appropriate horizontal momentum equations are those of planetary geostrophic balance and hydrostatic balance in each layer. This gives

$$\rho_n f v_n = \frac{\partial p_n}{\partial x}, \tag{10}$$

$$\rho_n f u_n = -\frac{\partial p_n}{\partial y}, \tag{11}$$

$$\rho_n g = -\frac{\partial p_n}{\partial z}, \tag{12}$$

$$\frac{\partial u_n}{\partial x} + \frac{\partial v_n}{\partial y} + \frac{\partial w_n}{\partial z} = 0. \tag{13}$$

where the final equation describes incompressibility. We can combine (10), (11) and (13) to derive the Sverdrup balance in each layer

$$\beta v_n = f \frac{\partial w_n}{\partial z}. \tag{14}$$

Integrating vertically over all layers, and using continuity of w_n at each density interface we obtain

$$\beta \sum_n v_n h_n = f w_e. \tag{15}$$

It will also prove useful to consider the evolution of the *potential vorticity* in each layer, f/h_n. Using incompressibility (13) to eliminate $\partial w/\partial z$ from the Sverdrup balance (14) and combining with the mass conservation relations (8-9) we obtain, after some algebra,

$$u_2 \frac{\partial}{\partial x}\left(\frac{f}{h_2}\right) + v_2 \frac{\partial}{\partial y}\left(\frac{f}{h_2}\right) = \frac{f}{h_2^2} w_e \Theta\left[y - y_2\right], \tag{16}$$

$$u_1 \frac{\partial}{\partial x}\left(\frac{f}{h_1}\right) + v_1 \frac{\partial}{\partial y}\left(\frac{f}{h_2}\right) = \frac{f}{h_1^2} w_e \Theta\left[y_2 - y\right]. \tag{17}$$

We use Θ to denote the Heaviside step function here,

$$\Theta\left[x\right] = \begin{cases} 1 & x > 0, \\ 0 & x < 0. \end{cases}$$

We note that potential vorticity is conserved in submerged layers, and it changes only due to Ekman pumping when the layer is in contact with the surface.

The horizontal pressure gradient in each layer can be related to the layer thicknesses. Vertically integrating the hydrostatic balance (12) and substituting into the geostrophic balance conditions (10-11) we obtain

$$f u_2 = -\frac{\partial}{\partial y}\left(\gamma_2 h\right), \qquad f v_2 = \frac{\partial}{\partial x}\left(\gamma_2 h\right), \tag{18}$$

$$f u_1 = -\frac{\partial}{\partial y}\left(\gamma_2 h + \gamma_1 h_1\right), \qquad f v_1 = \frac{\partial}{\partial x}\left(\gamma_2 h + \gamma_1 h_1\right), \tag{19}$$

where $h = h_1 + h_2$ and the relevant reduced gravities are

$$\gamma_1 = \frac{\rho_2 - \rho_1}{\rho_0} g, \qquad \gamma_2 = \frac{\rho_3 - \rho_2}{\rho_0} g. \tag{20}$$

2.1.2 Solution for the single moving layer

At large latitudes ($y > y_2$) layer 2 is in direct contact with the ocean surface and forms the only active layer, so that $h = h_2$. The depth-integrated Sverdrup balance (15) and geostrophic balance (18) then yield

$$\beta v_2 h_2 = f w_e, \qquad v_2 = \frac{\gamma_2}{f}\frac{\partial h_2}{\partial x}. \tag{21}$$

Eliminating v_2 we obtain a differential equation for h_2

$$\frac{\partial h_2^2}{\partial x} = 2\frac{f^2}{\beta \gamma_2} w_e. \tag{22}$$

There is no normal flow across the eastern boundary of the basin, and so $u_2 = 0$ at $x = x_e$. In general we can satisfy this condition by taking h_2 as a constant - however for our purposes it is sufficient to assume $h_2 = 0$ at $x = x_e$, so that upper layer has zero depth at the boundary. We ignore the details of the boundary conditions on the western boundary here, and assume that these are satisfied by an appropriate western boundary current similar to that obtained in the previous chapter. Integrating (22) gives the layer depth

$$h_2^2 = -2\frac{f^2}{\beta\gamma_2}\int_x^{x_e} w_e(x', y)\, dx' \qquad \text{for} \qquad y \geq y_2. \tag{23}$$

The entire solution is uniquely specified in terms of h_2 for $y \geq y_2$, with the horizontal velocities given by the conditions of geostrophic balance (18).

2.1.3 Solution for two moving layers

As we move closer to the equator layer 2 is subducted under layer 1 for $y \leq y_2$. The Ekman pumping then transfers to layer 1, so that the subducted layer is no longer driven directly by the surface forcing. The potential vorticity equation (16) for layer 2 then yields

$$\mathbf{u}_2 \cdot \nabla \left(\frac{f}{h_2}\right) = 0 \tag{24}$$

so that the potential vorticity is conserved on each streamline. We define a geostrophic streamfunction ψ_2, such that $fv_2 = \gamma_2 \partial\psi_2/\partial x$ and $fu_2 = -\gamma_2\partial\psi_2/\partial y$. We can then satisfy geostrophic balance (18) in layer 2 by setting $\psi_2 = h$. Hence we can write

$$\frac{f}{h_2} = Q_2(h) \tag{25}$$

for an arbitrary function Q_2, so that the potential vorticity is a function of streamline.

In order to determine the form of Q_2, we consider matching of the two solutions at the subduction point $y = y_2$, where $h_1 = 0$, $h = h_2$ and $f = f_2$. The constant f_2 is defined by

$$f_2 \equiv f_0 + \beta y_2. \tag{26}$$

Substituting these values into (25) we determine

$$Q_2\left[h_2(x, y_2)\right] = \frac{f_2}{h_2(x, y_2)} = \frac{f_2}{h(x, y_2)}, \tag{27}$$

so that we can write the potential vorticity as

$$\frac{f}{h_2(x, y)} = \frac{f_2}{h(x, y)}, \tag{28}$$

at any point in layer 2 with $y \leq y_2$. We can use the potential vorticity relation (28) to express the individual layer thicknesses in terms of f and h, giving

$$h_1 = \left(1 - \frac{f}{f_2}\right) h, \qquad h_2 = \frac{f}{f_2} h. \tag{29}$$

In order to determine the evolution of h we again use the depth integrated Sverdrup balance (15). The geostrophic balance relations (18-19) can be used to eliminate v_1 and v_2, so that we obtain

$$\frac{\partial}{\partial x}\left(h^2 + \frac{\gamma_1}{\gamma_2} h_1^2\right) = 2\frac{f^2}{\beta\gamma_2} w_e. \tag{30}$$

The appropriate boundary conditions are $h = h_1 = h_2 = 0$ at $x = x_e$, required to enforce no normal flow at the Eastern boundary. Integrating (30) gives

$$h^2 + \frac{\gamma_1}{\gamma_2} h_1^2 = -2 \frac{f^2}{\beta \gamma_2} \int_x^{x_e} w_e(x', y)\, dx' \qquad \text{for} \qquad y \leq y_2. \tag{31}$$

We eliminate h_1 in favor of h using (29) and obtain a solution for h in $y < y_2$, given by

$$h = \frac{\left(D_0^2\right)^{1/2}}{\left[1 + \frac{\gamma_1}{\gamma_2}\left(1 - \frac{f}{f_2}\right)^2\right]^{1/2}}, \tag{32}$$

where

$$D_0^2 \equiv -2 \frac{f^2}{\beta \gamma_2} \int_x^{x_e} w_e(x', y)\, dx' \geq 0. \tag{33}$$

The characteristic depth D_0 is a measure of the strength of the Ekman pumping which is forcing the circulation.

2.1.4 Structure of the full solution

We now look at the detailed structure of the solution for a particular example of Ekman pumping. Figure 5 shows calculated layer depths for an idealized Ekman pumping given by

$$w_e = \sin\left(\frac{\pi f}{f_0}\right). \tag{34}$$

The contours show the characteristic bowl structure as seen in field observations of the thermocline

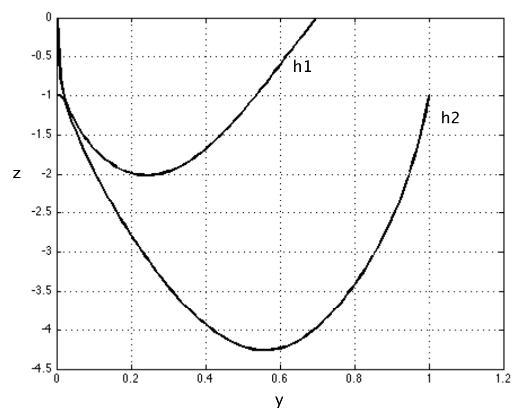

Figure 5: Plot of variation of the with latitude y of the density interfaces at $z = -h_1$ and z=$-h$ for $w_e = \sin(\pi f/f_0)$.

density structure (see figure 3.) The horizontal circulation is plotted in figure 6. The layer 1 circulation, confined to $y < y_2$, shows a similar qualitative circulation pattern to that given by the Sverdrup interior solution for a homogenous fluid. The layer 2 streamlines show the same

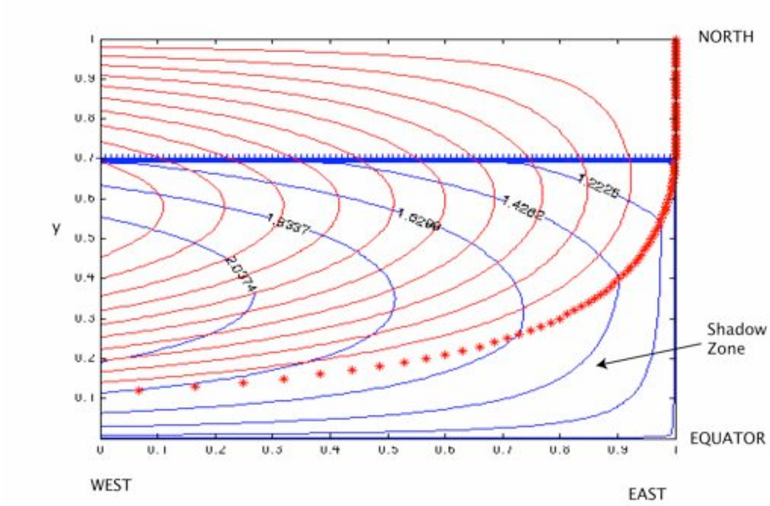

Figure 6: Plots of streamlines in layer 1 (blue curves) and layer 2 (red curves) in a square oceanic basin, for $w_e = \sin(\pi f/f_0)$. The blue dashed line shows the line $y = y_2$, where layer 2 subducts under the Northern most edge of layer 1. The red dotted curve marks the edge of a shadow zone in layer 2, with no flow to the South of this curve.

characteristic shape, except in a shadow zone towards the South-East of the basin. This shadow zone is an interesting prediction of the theory and can be explained as follows. The no normal flow boundary condition on the Eastern boundary requires that h_2 is constant on $x = x_e$. However, after layer 2 subducts and loses contact with the surface we have conservation of potential vorticity on streamlines ($\mathbf{u}_2 \cdot \nabla(f/h_2) = 0$ for $y < y_2$). Since f varies with y, we cannot satisfy the potential vorticity condition with constant h_2, unless $\mathbf{u}_2 = 0$ in a stagnant shadow zone adjacent to the boundary.

We now consider the behavior of the solution as we approach the equator at $y = 0$. If the wind stress τ is aligned in the x direction, we have

$$w_e = -\frac{\partial}{\partial y}\left(\frac{\tau}{\rho_0 f}\right) = -\frac{1}{\rho_0 f}\frac{\partial \tau}{\partial y} + \frac{\beta}{\rho_0 f^2}\tau, \tag{35}$$

and (33) becomes

$$D_0^2 = (x_e - x)\frac{2}{\rho_0 \gamma_2}\left(\frac{\partial \tau}{\partial y}\frac{f}{\beta} - \tau\right). \tag{36}$$

As $f \to 0$, D_0^2 approaches the finite value

$$D_0^2 = -\tau(x_e - x)\frac{2}{\rho_0 \gamma_2}. \tag{37}$$

At low latitudes the trade winds generate a negative shear stress $\tau < 0$, and so (32) implies that the layer thicknesses remain finite as $y \to 0$ and we approach the equator. However, if geostrophic balance is still to hold,

$$v_2 = \frac{\gamma_2}{f}\frac{\partial h}{\partial x}, \tag{38}$$

so that v_2 diverges as $f \to 0$. This singularity is clearly unphysical, and reflects the fact that a new physical balance must become important near the equator. We will resolve this problem in §2.1.6 by introducing an inertial boundary layer close to the equator, where the dynamical balances are modified.

2.1.5 Extensions and the continuous model

The simple model we have developed can be extended to improve the description of the physical processes at work. Rhines and Young (1982)considered how the wind driven circulation might impact directly on the lower layer and the ideas were developed further by Pedlosky and Young (1983) (see also Pedlosky, 1998). The extension towards a continuous model was considered by Huang (1989), who added a larger number of layers into the model. As the number of layers increases we approach a high resolution finite difference approximation to the continuous form of the solution. This solution also shows upwelling of isopycnals as we approach the equator.

2.1.6 The equatorial inertial boundary layer

Our current model of the thermocline breaks down as $y \to 0$ and we approach the equator, with geostrophic balance implying a divergence of the equator-ward velocity v_2 (we can also deduce a similar result for layer 1.) This singularity occurs due to the neglect of certain terms in the governing equations - in order to heal the singularity we must reintroduce the relevant terms to make sure we capture the correct physical balances. We return to the full non-linear inviscid governing equations in each layer, with mass conservation and horizontal momentum conservation in each layer yielding

$$\frac{\partial}{\partial x}(u_n h_n) + \frac{\partial}{\partial y}(v_n h_n) = 0, \tag{39}$$

$$u_n \frac{\partial u_n}{\partial x} + v_n \frac{\partial u_n}{\partial y} - \beta y v_n = -\frac{1}{\rho_0}\frac{\partial p_n}{\partial x}, \tag{40}$$

$$u_n \frac{\partial v_n}{\partial x} + v_n \frac{\partial v_n}{\partial y} + \beta y u_n = -\frac{1}{\rho_0}\frac{\partial p_n}{\partial y}. \tag{41}$$

We note that near to the equator the Coriolis parameter is approximately linear in y, so that $f = 2\Omega \sin\theta \approx \beta y$.

To determine the appropriate balances, we consider the scaling of all terms in the governing equations. We set

$$(x, y) = (Lx', ly'), \quad h = Hh', \quad (u, v) = U\left(u', \frac{l}{L}v'\right), \quad p = \rho_0 \beta l^2 U p', \tag{42}$$

where l, L and H are all lengthscales, and U is the appropriate velocity scale. Typically the basin width is $L \approx 1000$km and we will show that the width of the equatorial layer is $l \approx 100$km, so that $l \ll L$. Note that the scaling of the pressure has been chosen for a system where the pressure gradient will be of the same order as the coriolis acceleration. With these scalings in place, the non-dimensional forms of (39-41) are

$$\frac{\partial}{\partial x'}\left(u_n' h_n'\right) + \frac{\partial}{\partial y'}\left(v_n' h_n'\right) = 0, \tag{43}$$

$$\frac{U}{\beta l^2}\left(u_n'\frac{\partial u_n'}{\partial x'} + v_n'\frac{\partial u_n'}{\partial y'}\right) - y' v_n' = -\frac{\partial p_n'}{\partial x'}, \tag{44}$$

$$\frac{U}{\beta l^2}\frac{l^2}{L^2}\left(u_n'\frac{\partial v_n'}{\partial x'} + v_n'\frac{\partial v_n'}{\partial y'}\right) + y' u_n' = -\frac{\partial p_n'}{\partial y'}. \tag{45}$$

In order to avoid singular behavior of v as $y \to 0$, we need to include the non-linear inertia terms in the x-momentum balance (44). This requires that

$$U/\beta l^2 = \mathcal{O}(1). \tag{46}$$

The retention of some non-linearity reflects the fact that the relative component of vorticity becomes comparable to, and exceeds the planetary vorticity as we approach the equator. However, we can neglect the inertial terms in (45) due to the extra factor of $l/L \ll 1$, so that the y-momentum is in geostrophic balance. We have a loss of symmetry in a narrow region close to the equator, with only the x-component of inertia being important - this is sometimes called *semi-geostrophy*.

We require two further scaling relations in order to determine the depth scale H, boundary layer width l and velocity U uniquely in terms of the imposed physical scales. We assume the pressure will satisfy hydrostatic balance, so that

$$p \sim \rho_0 \gamma_2 H \sim \rho_0 U \beta l^2, \tag{47}$$

where the second balance is obtained from the direct scaling introduced for p. We determine a scale for H by assuming smooth matching of the depth of the thermocline outside of the internal boundary layer. This requires $H \sim D_0$, so that scaling of (36) yields

$$H^2 = \frac{\tau L}{\rho_0 \gamma_2}. \tag{48}$$

Combining (46-48) we obtain the lengthscales

$$l = \left(\frac{\gamma_2 \tau L}{\rho_0 \beta^4}\right)^{1/8}, \quad H = \left(\frac{\tau L}{\gamma_2 \rho_0}\right)^{1/2}, \quad U = \left(\frac{\gamma_2 \tau L}{\rho_0}\right)^{1/4}. \tag{49}$$

Using typical oceanic values of $\gamma \approx 0.01\mathrm{m\,s}^{-2}$, $L \approx 1000$km and $\tau \approx 0.01\mathrm{m}^2\,\mathrm{s}^{-2}$, we find that $l \approx 200$km, $H \approx 100$m and $U \approx 1\mathrm{ms}^{-1}$.

References

R. X. Huang. On the three dimensional structure of the wind-driven thermocline inthe North Atlantic. *Dyn. Atmos. and Oceans*, 15:117–159, 1989.

J. R. Luyten, J. Pedlosky, and H. Stommel. The ventilated thermocline. *J. Phys. Ocean.*, 13: 292–309, 1983.

J. Pedlosky. *Ocean Circulation Theory*, page 453. Springer Verlag, 1998.

J. Pedlosky and W. R. Young. Ventilation, potential vorticity homogenization and the structure of the ocean circulation. *J. Phys. Ocean.*, 13:2020–2037, 1983.